α-Synuclein–induced lysosomal dysfunction occurs through disruptions in protein trafficking in human midbrain synucleinopathy models

Joseph R. Mazzulli[a,b], Friederike Zunke[b], Ole Isacson[c], Lorenz Studer[d,e], and Dimitri Krainc[a,b,1]

[a]Department of Neurology, Massachusetts General Hospital, Harvard Medical School, MassGeneral Institute for Neurodegeneration, Charlestown, MA 02129; [b]The Ken and Ruth Davee Department of Neurology, Northwestern University Feinberg School of Medicine, Chicago, IL 60611; [c]Neuroregeneration Institute, McLean Hospital/Harvard Medical School, Belmont, MA 02478; [d]Center for Stem Cell Biology and Department of Neurosurgery, Memorial Sloan-Kettering Cancer Center, NY 10065; and [e]Developmental Biology Program, Memorial Sloan-Kettering Cancer Center, NY 10065

Edited by Thomas C. Südhof, Stanford University School of Medicine, Stanford, CA, and approved January 8, 2016 (received for review October 14, 2015)

Parkinson's disease (PD) is an age-related neurodegenerative disorder characterized by the accumulation of protein aggregates comprised of α-synuclein (α-syn). A major barrier in treatment discovery for PD is the lack of identifiable therapeutic pathways capable of reducing aggregates in human neuronal model systems. Mutations in key components of protein trafficking and cellular degradation machinery represent important risk factors for PD; however, their precise role in disease progression and interaction with α-syn remains unclear. Here, we find that α-syn accumulation reduced lysosomal degradation capacity in human midbrain dopamine models of synucleinopathies through disrupting hydrolase trafficking. Accumulation of α-syn at the cell body resulted in aberrant association with cis-Golgi–tethering factor GM130 and disrupted the endoplasmic reticulum-Golgi localization of rab1a, a key mediator of vesicular transport. Overexpression of rab1a restored Golgi structure, improved hydrolase trafficking and activity, and reduced pathological α-syn in patient neurons. Our work suggests that enhancement of lysosomal hydrolase trafficking may prove beneficial in synucleinopathies and indicates that human midbrain disease models may be useful for identifying critical therapeutic pathways in PD and related disorders.

synucleinopathies | protein trafficking | induced pluripotent stem cells | Parkinson's disease | long-term midbrain culture

Parkinson's disease (PD) is an age-dependent neurodegenerative disorder characterized by the accumulation of a synaptic protein, α-synuclein (α-syn), within Lewy bodies and neurites of the nervous system in the form of amyloid fibrils (1). Although the factors that convert α-syn from a normal soluble protein into insoluble amyloid aggregates are not known, recent studies have indicated that perturbations in cellular pathways that mediate the synthesis or degradation of α-syn may play a role. The formation of toxic aggregates in vitro is dramatically accelerated by increased α-syn concentration (2), a notion that is supported in vivo through PD patients that overproduce α-syn through *SNCA* gene triplication (trp) (3). In addition to aberrant synthesis, disruptions in protein clearance pathways have been linked to PD. For example, recent clinical, genetic, and pathological data demonstrate a linkage between the lysosomal storage disorder (LSD), Gaucher disease (GD), and synucleinopathies (4–6), suggesting that lysosomal dysfunction contributes to α-syn aggregation and PD pathogenesis (7).

Over 50 LSDs exist, and nearly all are characterized by neurodegeneration, emphasizing the importance of lysosomal function for neuronal health. Although biochemical identification of the storage material(s) has advanced our understanding of cellular dysfunction in these diseases, the mechanisms that lead to neurodegeneration are unknown. Previously, we demonstrated that the primary storage material of GD, glucosylceramide (GluCer), directly interacted with α-syn and promoted conformational conversion into pathogenic oligomeric species and amyloidogenic fibrils (8). We also showed that accumulated α-syn interfered with trafficking and activity of mutant or wild-type GCase (8).

In addition to lysosomal dysfunction, genetic analysis has indicated that defects in vesicular trafficking can lead to PD (9, 10). Interestingly, functional studies of trafficking proteins implicate their role in α-syn–mediated cell death (11–13). Whereas these studies imply that vesicle trafficking deficits may lead to α-syn accumulation, no studies have demonstrated a mechanistic linkage between these processes.

Here we show that α-syn impairs key vesicular trafficking components at the early secretory pathway, resulting in disrupted hydrolase trafficking and reduced lysosomal function. Expression of the small GTPase rab1a restored trafficking machinery and elevated lysosomal function, further suggesting that decreased trafficking of hydrolases represents the main mechanism of altered lysosomal function in synucleinopathies. Importantly, we confirmed our findings in induced pluripotent stem cell (iPSC)-derived midbrain neurons that naturally form amyloidogenic α-syn inclusions after culturing for hundreds of days. Our results suggest that improved trafficking of lysosomal hydrolases may be a viable target for the treatment of synucleinopathies.

Results

Lysosomal Dysfunction Induced by α-Synuclein Accumulation. To determine if a functional relationship exists between α-syn accumulation and the lysosomal system in human midbrain dopamine (DA) neurons, we measured the degradation rate of long-lived proteins in neurons that overexpress α-syn by lentiviral transduction. Midbrain neurons were generated from an extensively characterized iPSC line derived from a healthy control that was confirmed to lack PD-linked mutations (8), using a previously established differentiation protocol (14). Immunofluorescence analysis confirmed successful differentiation into midbrain neurons (*SI Appendix*, Fig. S1). Neurons were infected with lentiviral particles

Significance

There are currently no disease-altering therapies available for the treatment of Parkinson's disease or other age-related neurodegenerative disorders. Here, we find that enhancement of a single therapeutic pathway centered on hydrolase trafficking and lysosomal function potently reduces α-synuclein accumulation in human midbrain neurons. This work may lead to future treatments for age-related neurodegenerative diseases through the reduction of protein aggregates.

Author contributions: J.R.M. and D.K. designed research; J.R.M. and F.Z. performed research; J.R.M., O.I., and L.S. contributed new reagents/analytic tools; J.R.M., F.Z., and D.K. analyzed data; and J.R.M., F.Z., and D.K. wrote the paper.

The authors declare no conflict of interest.

This article is a PNAS Direct Submission.

[1]To whom correspondence should be addressed. Email: krainc@northwestern.edu.

This article contains supporting information online at www.pnas.org/lookup/suppl/doi:10.1073/pnas.1520335113/-/DCSupplemental.

to express human WT α-syn, and Western blot analysis indicated a two-to-threefold elevation in protein levels (Fig. 1*A*). To determine the effect of α-syn aggregation on lysosomal function, we also infected DA neurons with an α-syn deletion mutant, Δ71–82, lacking the mostly hydrophobic domain responsible for amyloid fibril formation (15, 16). Lenti-WT-α-syn–infected DA neurons showed a decline in long-lived proteolysis rates compared with vector (Fig. 1*B*), and comparison of WT-α-syn–expressing neurons with the Δ71–82 mutant indicated that lysosomal dysfunction is exacerbated by aggregation-dependent mechanisms (Fig. 1*B*).

To confirm the effects of α-syn accumulation on the lysosomal system using a more natural overexpression model, we generated and characterized PD midbrain neurons that overexpress α-syn through genetic triplication (*SNCA* trp) (*SI Appendix*, Fig. S2) (3). Two *SNCA* trp lines were used throughout this study (PD-1 and PD-2) and compared with neurons from three different healthy control individuals (ctrl-1, ctrl-2, and ctrl-3). Additionally, we used a previously characterized line that accumulates α-syn as a result of *GBA1* mutations (N370S/c.84dupG) (8). Extensive analysis of the culture population indicated similar expression of midbrain markers (β-III tubulin, TH, FOXA2, and LMX1a) between lines that persisted for 330 d (*SI Appendix*, Figs. S3 and S4).

Immunostaining analysis revealed that α-syn was localized to synapses in control and patient neurons, however, began accumulating at the cell body of *SNCA* trp neurons at day 60 (*SI Appendix*, Fig. S5). Pathological analysis indicated the presence of amyloidogenic inclusions in cell bodies and neurites by day 90 (*SI Appendix*, Fig. S6), as well as accumulation of soluble oligomeric and insoluble species that persisted for 330 d (Fig. 1*C* and *SI Appendix*, Fig. S7). This indicates that the midbrain patient model recapitulates several features of PD brain.

We next sought to determine if α-syn aggregates naturally formed by *SNCA* trp result in lysosomal dysfunction through measuring long-lived protein degradation. The dependability of the assay for detecting changes in patient lines was established by comparing proteolysis rates of three healthy controls. We found that all lines responded very similarly to lysosomal inhibitors (*SI Appendix*, Fig. S8). Next, we compared proteolysis rates of controls vs. *SNCA* trp midbrain neurons and found no statistical differences until d180 when patient lines showed rates that were ~50% lower than controls, although data at d110 approached significance at $P = 0.09$ (Fig. 1*D*). We also found reduced proteolysis in GD midbrain neurons, compared with both PD and control lines at d110 (Fig. 1*D*). Degradation of short-lived proteins that are mainly degraded by the proteasome was measured and indicated no difference between control and patient lines at d180 (*SI Appendix*, Fig. S9*A*). Consistent with lysosomal dysfunction, increased lysosomal mass was detected in PD and GD neurons. Importantly, this effect was partially rescued by lenti-shRNA knockdown of α-syn in both PD and GD lines (*SI Appendix*, Fig. S9 *B–D*). Together with data in Fig. 1, this indicates that lysosomal dysfunction likely occurs as a downstream consequence of α-syn accumulation that is partially reversible upon α-syn reduction.

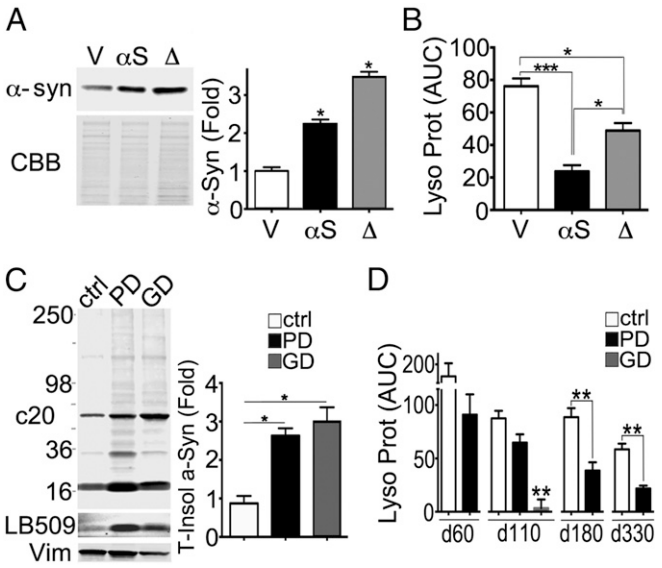

Fig. 1. Compromised lysosomal function in human midbrain DA neurons that accumulate α-syn. (*A*) Western blot of α-syn (antibody syn211) showing overexpression of human WT α-syn (αS) or aggregation-deficient Δ71–82 mutant (Δ) by lentiviral infection [multiplicity of infection (moi) 5, days post infection (dpi) 14] compared with empty vector (V) in midbrain DA neurons derived from a healthy control. Coomassie Blue (CBB) staining of the gel indicates loading. (*Right*) Quantification of normalized α-syn levels ($n = 3$, $^*P < 0.05$ compared with Vect). (*B*) Lysosomal proteolysis (Lyso Prot) in midbrain DA neurons was assessed by a radioactive pulse–chase assay ($n = 4$, values are the mean ± SEM, $^*P < 0.05$, $^{***}P < 0.001$). Area under curve (AUC) obtained from kinetic data of protein degradation over time. (*C*) Western blot of Triton-X 100 insoluble α-syn from d90 PD (*SNCA* trp) or GD (*GBA1* N370S/c.84dupG) midbrain neurons. Molecular weight (MW) in kDa is shown. Vimentin (Vim) was used as a loading control. (*Right*) Quantification of insoluble α-syn (LB509) normalized to vim ($n = 4$, $^*P < 0.05$). (*D*) Quantification of lysosomal proteolysis from living neurons at different incubation times ($n = 5$, $^{**}P < 0.01$). Values are the mean ± SEM. ANOVA with Tukey's post hoc test was used for *A–C*. Student's *t* test was used for *D*.

α-Synuclein Impedes Lysosomal Function Through Reducing Hydrolase Activity. To gain a mechanistic understanding of how α-syn accumulation leads to lysosomal dysfunction, we considered the possibility that α-syn reduces the activity of hydrolases within the lysosomal compartment. This hypothesis is based on our previous finding that α-syn reduces GCase activity in lysosomal fractions when measured in vitro (8). To test this, we measured the activity of cathepsin B using a live-cell assay capable of distinguishing lysosomal vs. nonlysosomal activity (*SI Appendix*, section 2g). Using this approach, we found a significant reduction in lysosomal cathepsin B activity in PD and GD patient neurons compared with controls (*SI Appendix*, Fig. S10).

In addition to cathepsin B, we observed reduced activity of other nonprotein-degrading lysosomal enzymes, including GCase, β-galactosidase (β-gal), and hexosaminidase (hex), within acidic subcellular compartments, whereas total activity (lysosomal + nonlysosomal) was not changed (Fig. 2 *A* and *B*). The expression of aggregation-deficient Δ71–82 α-syn, or aggregation-prone poly-Q-huntingtin, had a minimal effect on lysosomal GCase activity, indicating that inhibition resulted specifically from α-syn aggregation (Fig. 2*A*). Enzymatic deficiency in lysosomal compartments was observed in three different control lines infected to overexpress α-syn (Fig. 2 *A* and *B* and *SI Appendix*, Fig. S11), as well as patient lines that naturally accumulate α-syn (Fig. 2 *C–F*), demonstrating a reproducible effect. GD lines exhibited little GCase activity as expected, but also demonstrated reduced activity of other hydrolases, including β-gal, Hex, and Sulfatase (Fig. 2 *C–F*).

To confirm enzymatic deficiency in a separate PD line, we generated midbrain neurons from an idiopathic PD (iPD) patient that accumulates α-syn (*SI Appendix*, Fig. S12 *A–C*). Similar to *SNCA* trp and GD neurons, iPD neurons demonstrated a reduction in GCase activity specifically within acidic subcellular compartments (*SI Appendix*, Fig. S12*D*).

Importantly, reduction of α-syn in both *SNCA* trp and GD lines by shRNA knockdown increased the activity of hydrolases within the lysosomal compartment, indicating that hydrolase activity is specifically affected by α-syn accumulation (Fig. 2 *G* and *H*). Together, the data suggest that α-syn accumulation results in reduced enzymatic activity of multiple lysosomal hydrolases, leading to lysosomal dysfunction.

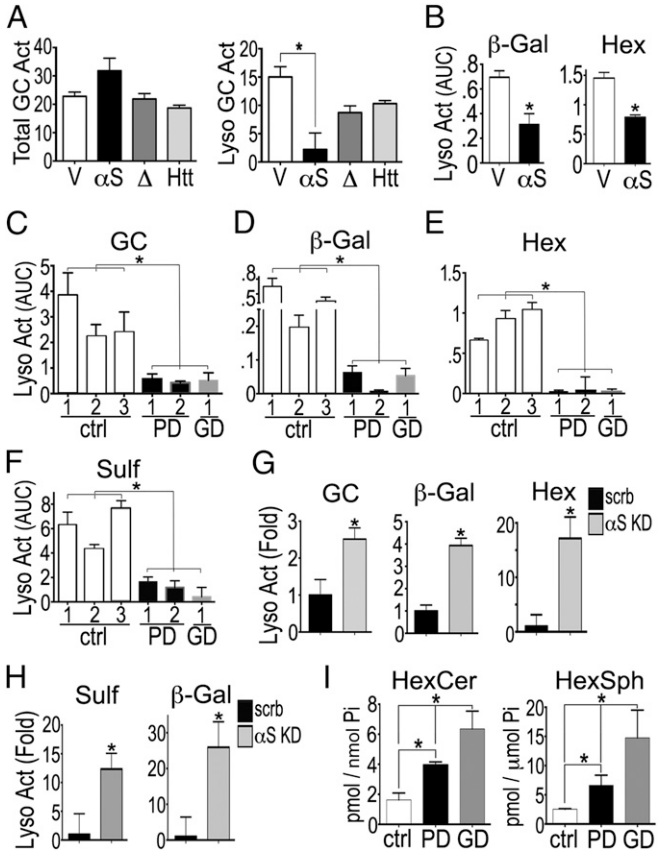

Fig. 2. Reduced hydrolase activity in human midbrain DA neurons that accumulate α-syn. (*A*) Total enzymatic activity (Total GC Act) of GC was assessed in living control midbrain neurons derived from a healthy control (C1) infected with empty vector (V), or lenti-α-syn (αS) (moi 5, dpi 14) at day 120 through quantifying the degradation of a fluorescent-tagged substrate (PFB-FD-Glu). (*Right*) Activity within acidic lysosomal compartments (Lyso GC Act) was determined by quantifying the response to bafilomycin A1 ($n = 4$). Expression of Δ71–82 α-syn (Δ) and poly Q-expanded huntingtin (Htt) (548-72Q) were used as specificity controls. (*B*) Lysosomal activity of β-gal and hexosaminidase (hex) was measured as described in *A* ($n = 4$). AUC obtained from kinetic data of substrate degradation over time. (*C–F*) Lysosomal enzyme activity in *SNCA* trp (PD) or *GBA1* N370S/c.84dupG (GD) patient lines was measured as described in *A* and *B* at day 180 ($n = 4$). (*G* and *H*) Lysosomal enzyme activity in *SNCA* trp (PD) (*G*) or GD (*H*) midbrain neurons infected with lenti-shRNA constructs to knockdown α-syn (αS KD) compared with scrambled shRNA sequences (scrb) ($n = 4$). (*I*) Measurement of hexosylceramide (HexCer) and hexosylsphingosine (HexSph) levels analyzed at d180 ($n = 4$). Lipids were normalized to inorganic phosphate (Pi). For all quantifications, values are the mean ± SEM. $^*P < 0.05$. ANOVA with Tukey's post hoc test was used for *A*, *C–F*, and *I*. Student's *t* test was used for *B*, *G*, and *H*.

We next determined whether the decline in enzymatic activity was sufficient to induce substrate accumulation in patient neurons. Quantitative analysis of GCase substrates, including total hexosylceramide and hexosylsphingosine species, by mass spectrometry revealed nearly twofold elevation in PD (*SNCA* trp) neurons and an ∼fourfold elevation in GD neurons when incubated for 180 d (Fig. 2*I*). Separation of hexosyl species into glucosyl and galactosylceramide showed that both metabolites were significantly elevated in PD neurons, whereas ceramide levels decreased (*SI Appendix*, Fig. S13). In addition, we found no change in dihydroceramide levels, a nonlysosomal lipid species (*SI Appendix*, Fig. S13, *Right*). Thus, it appears that chronic lysosomal hydrolase deficiency induced by α-syn accumulation in long-term cultures is sufficient to induce lipid accumulation in PD midbrain neurons, even in the context of WT GCase expression.

Disrupted Hydrolase Trafficking Induced by α-Synuclein Accumulation. Because the live-cell lysosomal assay indicated a specific reduction of activity within lysosomes but no change in total cellular activity (Fig. 2*A*), we considered the possibility that α-syn results in enzyme mistargeting. This notion is consistent with previous data showing that α-syn disrupts vesicular trafficking (17–20). To test this, hydrolase maturation was examined by quantifying the levels of mature and immature hydrolase forms that migrate differently on SDS/PAGE gels due to compartment-specific glycosylation and protein cleavage (21). Measurement of mature:immature hydrolase ratios of Hex A and B in control midbrain neurons infected with lenti-WT α-syn indicated a decline in enzyme maturation, compared with empty vector and Δ71–82 α-syn–infected neurons (Fig. 3*A*). Enzyme localization studies revealed enzyme accumulation in pre-Golgi compartments [COPII endoplasmic reticulum (ER)-to-Golgi transport vesicles labeled with anti-sec23 antibodies] that was reversible upon reduction of α-syn expression (Fig. 3*B*). Extracts from patient neurons showed reduced maturation of GCase, β-gal, iduronate-2-sulfatase (I-2-sulf), and hex A (Fig. 3*C*), an effect that was reversible by lenti-mediated knockdown of α-syn (*SI Appendix*, Fig. S14). Hydrolase maturation was not altered by lysosomal inhibition alone (baf A1), indicating a specific trafficking defect induced by α-syn (*SI Appendix*, Fig. S15).

We also measured hydrolase maturation responses to well-established trafficking inhibitors that act at the level of the ER (tunicamycin) or Golgi (brefeldin A, BFA) in H4 cells. These compounds did not inhibit hydrolase maturation as effectively in high-expressing α-syn cells (−dox) compared with low-expressing cells (+dox) (*SI Appendix*, Fig. S16), suggesting that α-syn alters enzyme maturation through the early secretory pathway. Consistent with this, we found accumulation of COPII transport vesicles in α-syn H4 cells that was reversible upon reduced expression of α-syn (*SI Appendix*, Fig. S17). In patient neurons that accumulate α-syn at the cell body, we noted aberrant colocalization of α-syn with vesicle-tethering factor GM130 within fragmented, vesicular Golgi structures (Fig. 3*D*). GM130-α-syn colocalization was never observed in control neurons. Golgi fragmentation did not occur from lysosomal inhibition by baf A1, indicating a specific effect by α-syn (*SI Appendix*, Fig. S18). Together, this indicates that α-syn likely disrupts hydrolase trafficking at the cis-Golgi through aberrant association with fusion machinery.

A key regulator of ER-Golgi trafficking is rab1a (22), and previous studies showed that rab1a could rescue α-syn–induced neurodegeneration (17). Therefore, we determined if α-syn interacted with or altered rab1a levels in cells that accumulate α-syn. We found no difference in rab1a between control and patient neurons, and coimmunoprecipitations failed to detect an interaction of α-syn with rab1a (*SI Appendix*, Fig. S19). However, immunostaining analysis indicated that α-syn altered the location of rab1a from its normal perinuclear ER-Golgi localization to a more diffuse pattern (*SI Appendix*, Fig. S20). Because these data indicated perturbations in rab1a, we next determined if rab1a overexpression resulted in restoration of protein trafficking and lysosomal function in patient neurons. Lenti-rab1a expression restored Golgi structure and improved hydrolase maturation and activity in both lenti-α-syn–infected control lines and patient lines at 5 dpi (Fig. 4 *A–F* and *SI Appendix*, Fig. S21). Rab1a overexpression in healthy control neurons did not enhance lysosomal activity (Fold Change: Vector = 1.0 ± 0.17, Rab1a = 0.84 ± 0.07; $n = 3$, values are the mean ±SEM), indicating that rab1a restores a deficient pathway in patient lines as opposed to elevation of an alternate pathway unrelated to α-syn toxicity. At later time points after rab1a overexpression (dpi 14), we found that lysosomal enhancement by rab1a reduced the accumulation of α-syn within cell

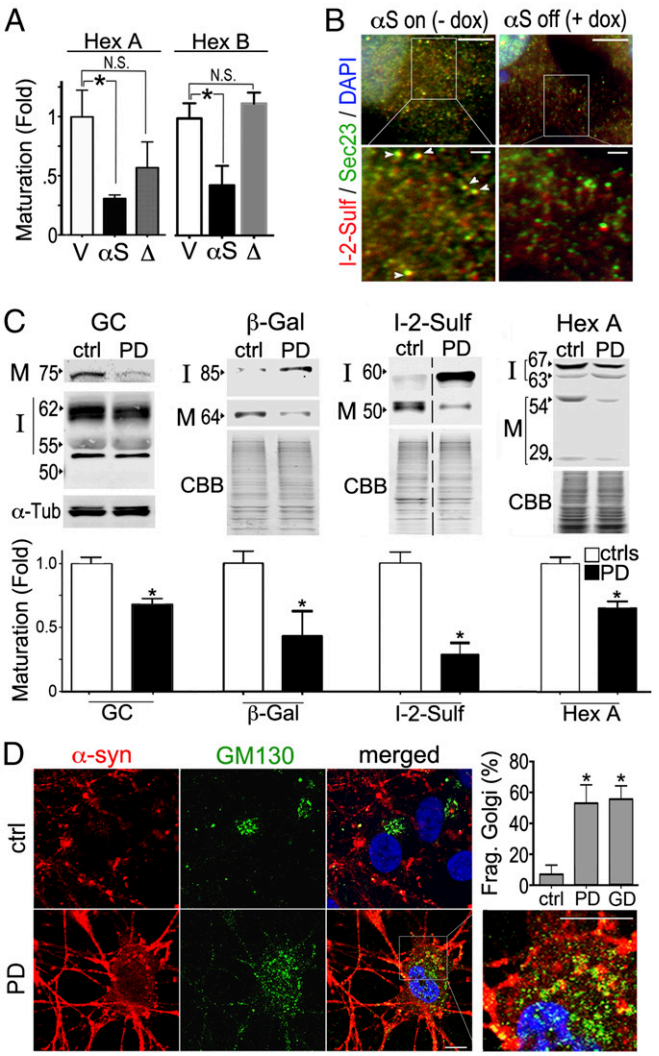

Fig. 3. Disrupted hydrolase trafficking in cells that accumulate α-syn. (*A*) Control neurons were infected to overexpress WT α-syn (αS) or Δ71–82 mutant (Δ), and maturation of Hex A and B was assessed by quantifying mature: immature ratios detected by Western blot ($n = 4$, $^*P < 0.05$, N.S., not significant). (*B*) Immunofluorescence analysis of inducible H4 human neuroglioma cells shows accumulation of I-2-Sulf in pre-Golgi COPII vesicles (stained with anti-Sec23 antibodies) that is reversible upon reduction of α-syn expression with doxycycline (dox). [Scale bar, 5 μm, or 1 μm (*Inset*).] (*C*) Maturation of GC, β-gal, iduronate-2-sulfatase (I-2-Sulf), and Hex A at day 180 PD (*SNCA* trp) neurons analyzed by Western blot. (I, immature; M, mature.) Plotted below are quantifications of mature:immature ratios ($n = 3$–4, $^*P < 0.05$). Shown is MW in kDa. The dashed line indicates cropped-out replicates but were ran on the same gel. Coomassie Blue (CBB) or αtubulin was used as a loading control. Mature and immature hydrolase forms shown are from the same blot, but separate exposures were required to avoid saturating band intensities. (*D*) DA neurons were immunostained with antibodies against GM130, located at the cis-Golgi (green). α-Syn puncta accumulated at the cell body (red) was partially colocalized with GM130. Nuclei were detected with DAPI (blue). (Scale bars, 5 μm.) The percentage of neurons with fragmented Golgi was quantified in the graph ($n = 4$, $^*P < 0.05$ compared with control line). ANOVA with Tukey's post hoc test was used for *A* and *D*. Student's *t* test was used for *C*.

bodies of *SNCA* trp neurons at d330 and improved neuroviability (Fig. 4 *G* and *H* and *SI Appendix*, Fig. S21 *D* and *E*). Together, the data indicate that α-syn–induced lysosomal dysfunction occurs through perturbations in hydrolase trafficking at the early secretory pathway that is reversible by rab1a.

Discussion

Loss-of-function mutations in metabolic genes have recently been recognized as important risk factors for common neurodegenerative disorders such as Parkinson's and Alzheimer's disease (23, 24). A well-established example of this is the relationship between GD and PD, where mutations in *GBA1* lead to increased risk for PD (6). Our previous work showed that loss-of-function mutations in *GBA1* lead to α-syn accumulation and neurodegeneration, an observation that has since been confirmed and extended by other groups (8, 25–29). Here, we used human midbrain neurons to examine the interaction between α-syn, lysosomes, and trafficking components in a more comprehensive manner. Human midbrain synucleinopathy models were generated through lentiviral overexpression of α-syn in control cultures, or through the generation of patient lines harboring PD-causing mutations. Our data from patient lines suggest that chronic overexpression of α-syn results in the accumulation of soluble oligomers, as well as insoluble amyloidogenic aggregates within cell bodies and neurites, recapitulating several features of PD brain (Fig. 1 and *SI Appendix*, Figs. S5–S7).

The stability of the culture system allowed us to incubate patient neurons for several hundred days and validate pathogenic changes in the lysosomal system that result from naturally occurring mutations leading to α-syn accumulation. We show that α-syn accumulation did not change total cellular enzymatic activity of hydrolases, but caused a significant decline specifically within acidic subcellular compartments of living neurons (Fig. 2*A*). Previous studies using in vivo synucleinopathy models did not detect changes in enzymatic activity when measured from whole-brain samples (30). Although valuable, these studies may have been complicated by the use of heterogeneous populations of neuronal and nonneuronal cells used to ascertain enzymatic activity. This is particularly important to consider when measuring α-syn–mediated cellular dysfunction from mixtures of cells because α-syn is mainly expressed and accumulates in neurons but not glia in PD (31, 32). The culture system and live-cell lysosomal assay used here allow for the detection of compartment-specific enzymatic activity within homogenous neuronal cultures, eliminating confounding factors that occur from mixed-cell populations and artificial activation of enzymes present in activity assay buffers. The fact that α-syn did not affect total activity but did induce a compartment-specific enzymatic dysfunction suggests that α-syn may not directly inhibit enzymes, but disrupts their subcellular location.

The effect of α-syn on lysosomal function was reproduced in seven different neuronal lines, including three lines transduced to overexpress α-syn by lentiviral infection, three additional synucleinopathy patient lines that accumulate α-syn as a result of natural mutations (two *SNCA* trp and one *GBA1*), and one iPD line (Fig. 2 and *SI Appendix*, Figs. S11 and S12). In patient lines, we found that α-syn knockdown restored enzyme trafficking and activity, indicating that these effects are mediated specifically by α-syn accumulation (Fig. 2 *G* and *H* and *SI Appendix*, Fig. S9 *C* and *D*). Interestingly, α-syn knockdown improved the activity of sulfatase and β-gal in *GBA1* mutant lines (Fig. 2*H*), suggesting that α-syn plays a role in the secondary lysosomal dysfunction that occurs in GD. The finding that Δ71–82 α-syn, a mutant protein with an extremely slow propensity to aggregate (16), did not alter lysosomal function to the same extent as WT α-syn indicates that amyloid or intermediate species exacerbate the effect (Figs. 1*B* and 2*A*).

Importantly, we found that enzymatic dysfunction in synucleinopathy models was sufficient to induce lipid substrate accumulation, even in the context of wild-type hydrolase expression (Fig. 2*I* and *SI Appendix*, Fig. S13). Recent studies have shown that elevations in GCase substrates can be documented when measured from certain circumscribed brain regions of PD patients (with or without *GBA1* mutations) (33). However, other studies of *GBA1* heterozygous mice have shown no changes in

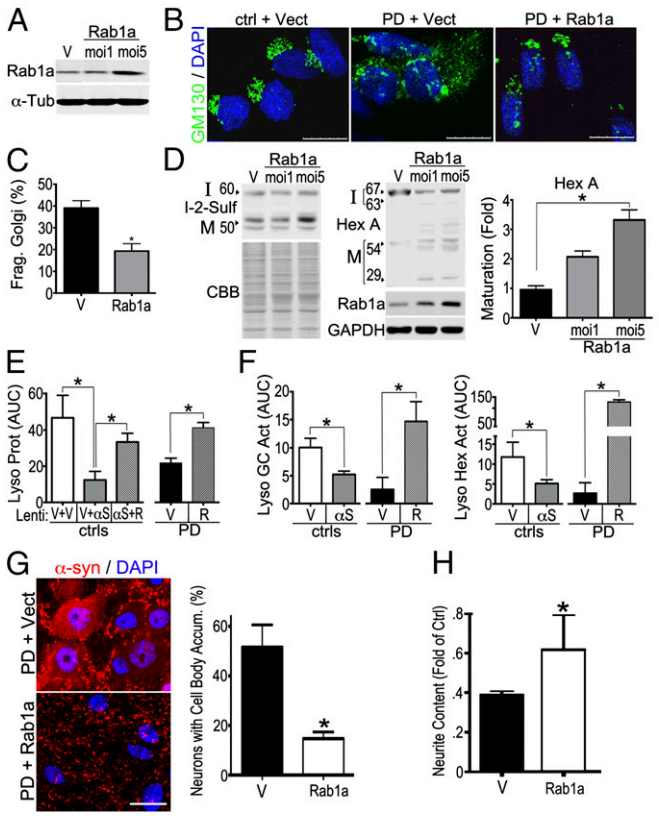

Fig. 4. Rab1a rescues lysosomal function by improving hydrolase trafficking and reduces pathological α-syn in human midbrain synucleinopathy models. (*A*) Western blot analysis of PD (*SNCA* trp) neurons infected to overexpress rab1a at moi 1 and 5. a-Tubulin was used as a loading control. (*B*) Analysis of Golgi structure in PD patient neurons by GM130 immunostaining (green) at d240 after rab1a expression (dpi 5, moi 5). (Scale bar, 10 μm.) (*C*) Quantification of fragmented Golgi of PD neurons ($n = 4$, $^*P < 0.05$). (*D*) Analysis of I-2-sulfatase and Hex A maturation in PD neurons treated with lenti-rab1a (moi 5, dpi 5) by Western blot. (I, immature; M, mature.) GAPDH or Coomassie blue (CBB) were used as loading controls. (*Right*) Quantification of Hex A maturation ($n = 3$, $^*P < 0.05$). (*E*) Lysosomal proteolysis (Lyso Prot) was analyzed in transduced control neurons overexpressing two empty vectors (V + V), V+ WT α-syn (αS), or WT α-syn + rab1a (αS + R), at d330. Proteolysis was also measured in PD (*SNCA* trp) neurons transduced with either empty vector (V) or rab1a (R) lentivirus ($n = 6$, $^*P < 0.05$). AUC obtained from kinetic data of protein degradation over time. (*F*) Analysis of lysosomal GC and Hex activity in living control neurons transduced to overexpress WT α-syn, or PD (*SNCA* trp) neurons overexpressing rab1a at day 200 ($n = 9$ ctrls, $n = 6$ PD, $^*P < 0.05$). (*G*) Immunostaining analysis of α-syn (red) in PD midbrain neurons at day 330 showing reduction of α-syn within cell bodies and restoration of synaptic puncta by rab1a (moi 5, dpi 14). (*Right*) Quantification of neurons with α-syn cell body accumulation ($n = 4$, $^*P < 0.05$). (Scale bar, 10 μm.) (*H*) Neuroviability was assessed by measuring neurofilament content at d330 (moi 5, dpi 14) ($n = 6$, $^*P < 0.05$). ANOVA with Tukey's post hoc test was used for *D*. (*Left*) Control graphs of *D*. Student's *t* test was used for *C*, *E* (PD graphs), *F*, and *G*. For all quantifications, values are the mean ± SEM.

substrate levels when measured from whole brain samples, suggesting that residual enzymatic activity may be sufficient to prevent neuronal substrate accumulation (26). It is possible that nonaffected cells, including neurons free of α-syn pathology and glial cells, mask detectable changes in diseased neurons. An important distinction with our studies is the use of homogeneous populations of DA neurons that exhibit pathological α-syn accumulation in 30–50% of neurons (*SI Appendix*, Fig. S4–S6). Our data suggest that α-syn aggregates in brains of *GBA1* mutant carriers can provide an additional pathological insult that, in addition to *GBA1* heterozygote mutations, contribute to lysosomal deficiency of GCase leading to substrate accumulation. Although not all carriers of *GBA1* mutations will develop PD, the penetrance is likely dictated by a combination with other mutations and/or environmental factors that may contribute to α-syn accumulation. Enzyme deficiency and lipid accumulation induced by α-syn accumulation in cells that express WT GCase (Fig. 2*I*) suggests that this mechanism may be relevant for both *GBA1* WT and mutant carriers that develop Lewy inclusions.

Consistent with previous work (17, 20, 34), our data indicate that α-syn disrupts vesicular trafficking at the early secretory pathway. We extended these studies to demonstrate that α-syn disrupts hydrolase trafficking and lysosomal function that can potentially lead to augmented α-syn accumulation. Previous studies indicated that α-syn mutants or oxidized aggregated forms of the protein can impede substrate delivery into lysosomes through blocking LAMP2a, thereby disrupting chaperone-mediated autophagy (CMA) (35, 36). Although we cannot exclude the possibility that LAMP2a blockade contributes to proteolysis deficits observed here (Fig. 1 *B* and *D*), we observe enzyme accumulation in pre-Golgi compartments and reduced lysosomal activity of both protein-degrading and nonprotein-degrading enzymes using substrates that do not depend on CMA (Figs. 2 *A*–*F* and 3*B*). Importantly, the trafficking effects were not observed under conditions of lysosomal inhibition by baf A1 (*SI Appendix*, Figs. S15 and S18), indicating that disrupted hydrolase trafficking in patient neurons cannot be explained by direct lysosomal inhibition. In addition, we found that α-syn induced the accumulation of ER-Golgi COPII transport vesicles, suggesting a blockade in vesicle fusion at the cis-Golgi (*SI Appendix*, Fig. S17). Previous studies have found that rab1a–GM130 interactions are required for COPII vesicle fusion to the cis-Golgi (37). Our data suggest that aberrant association of α-syn with GM130 disrupts COPII vesicle fusion through altering the ER-Golgi location of rab1a (*SI Appendix*, Fig. S20), resulting in Golgi fragmentation (Fig. 3*D* and *SI Appendix*, Fig. S18). Overexpression of rab1a restored Golgi structure and promoted hydrolase trafficking and function (Fig. 4 *A*–*F* and *SI Appendix*, Fig. S21). Because a key function of rab1a is to promote vesicle tethering at the cis-Golgi, it is possible that rab1a overexpression enhanced hydrolase trafficking in patient neurons by providing more vesicle-fusing opportunities at acceptor membranes. Importantly, rab1a-mediated restoration of hydrolase trafficking was sufficient to reduce pathological α-syn and improve neuroviability in neurons derived from three distinct synucleinopathy patients (*SNCA* trp, GD, and iPD) (Fig. 4 *G* and *H* and *SI Appendix*, Fig. S21). This suggests that enhancing protein trafficking can reverse the pathogenic link between α-syn and lysosomal dysfunction. Once enzymes are correctly targeted to lysosomes and function is restored, α-syn reduction may occur through CMA or macroautophagy-mediated degradation of α-syn (35, 38, 39). In addition, the restoration of GCase activity by rab1a will likely reduce GluCer accumulation, thereby reducing the interaction with α-syn oligomers and rendering them amenable to degradation by lysosomal proteases. Recently identified PD-linked mutations that disrupt vesicular trafficking imply the importance of this pathway for PD and related synucleinopathies (9). Our data indicate that therapies focused on enhancement of the trafficking machinery of lysosomal hydrolases may prove beneficial in disorders characterized by accumulation of α-syn.

Materials and Methods

SI Appendix provides details and additional methods not listed below.

Proteolysis in Live Cells. Long-lived proteolysis rates within lysosomes was determined by quantifying the response to lysosomal inhibitors leupeptin and ammonium chloride, which inhibit lysosomes independently of the autophagic substrate delivery system. The assay was done as described previously (8) using tritium-labeled leucine (Perkin–Elmer, www.perkinelemer.com) to label long-lived proteins, followed by a chasing period of 24 h. Aliquots of culture media

were sampled over time, and percentage of labeled acid-soluble amino acids was used as an indication of proteolysis. Normalized radioactivity was graphed over time and analyzed by quantifying the area under the curves (AUC) corresponding to control and inhibited conditions (leupeptin at 100 μM 72 h, NH_4Cl at 5 mM 24 h). Lysosomal proteolysis was calculated as the difference between control and inhibited AUC curves. Differences in AUC values were graphed in column format ($n = 4$ per condition, repeated in five separate sets of differentiated cultures).

Enzyme Activity Assays and Lysosomal Mass Assessment. Activity was assessed in living neurons seeded in 96- well plates by incubating cultures with fluorescent-conjugated hydrolase substrates (*SI Appendix*) for 30 min to load cells, followed by a substrate washout. Substrate degradation was measured in a microplate reader over 3 h. Activity in acidic compartments was achieved through measuring the response to bafilomycin A1 and normalized to lysosomal mass (measured by cascade dextran blue fluorescence). Details can be found in *SI Appendix*.

ACKNOWLEDGMENTS. We thank Jessica Sadick and Sohee Jeon for technical assistance. This work was supported in part by the Human Embryonic and Induced Pluripotent Stem Cell Facility at Northwestern University and NIH core support Grant P30 NS081774. Lipidomics were supported in part by the Lipidomics Shared Resource, Hollings Cancer Center, Medical University of South Carolina (P30 CA138313), and the Lipidomics Core in the South Carolina Lipidomics and Pathobiology Center of Biomedical Research Excellence, Department Biochemistry, Medical University of South Carolina (P20 RR017677). This research was supported by the National Institute of Neurological Disorders and Stroke Grant R01NS076054 (to D.K.), R01NS092823 (to J.R.M.), and U24NS078338 (to O.I., D.K., and L.S.).

1. Spillantini MG, et al. (1997) Alpha-synuclein in Lewy bodies. *Nature* 388(6645): 839–840.
2. Wood SJ, et al. (1999) alpha-synuclein fibrillogenesis is nucleation-dependent. Implications for the pathogenesis of Parkinson's disease. *J Biol Chem* 274(28):19509–19512.
3. Singleton AB, et al. (2003) alpha-Synuclein locus triplication causes Parkinson's disease. *Science* 302(5646):841.
4. Neudorfer O, et al. (1996) Occurrence of Parkinson's syndrome in type I Gaucher disease. *QJM* 89(9):691–694.
5. Wong K, et al. (2004) Neuropathology provides clues to the pathophysiology of Gaucher disease. *Mol Genet Metab* 82(3):192–207.
6. Sidransky E, et al. (2009) Multicenter analysis of glucocerebrosidase mutations in Parkinson's disease. *N Engl J Med* 361(17):1651–1661.
7. Nixon RA (2013) The role of autophagy in neurodegenerative disease. *Nat Med* 19(8): 983–997.
8. Mazzulli JR, et al. (2011) Gaucher disease glucocerebrosidase and α-synuclein form a bidirectional pathogenic loop in synucleinopathies. *Cell* 146(1):37–52.
9. Hunn BH, Cragg SJ, Bolam JP, Spillantini MG, Wade-Martins R (2015) Impaired intracellular trafficking defines early Parkinson's disease. *Trends Neurosci* 38(3):178–188.
10. Martin I, Kim JW, Dawson VL, Dawson TM (2014) LRRK2 pathobiology in Parkinson's disease. *J Neurochem* 131(5):554–565.
11. Tang FL, et al. (2015) VPS35 in dopamine neurons is required for endosome-to-Golgi retrieval of Lamp2a, a receptor of chaperone-mediated autophagy that is critical for α-Synuclein degradation and prevention of pathogenesis of Parkinson's disease. *J Neurosci* 35(29):10613–10628.
12. Dhungel N, et al. (2015) Parkinson's disease genes VPS35 and EIF4G1 interact genetically and converge on α-synuclein. *Neuron* 85(1):76–87.
13. Lin X, et al. (2009) Leucine-rich repeat kinase 2 regulates the progression of neuropathology induced by Parkinson's-disease-related mutant alpha-synuclein. *Neuron* 64(6):807–827.
14. Kriks S, et al. (2011) Dopamine neurons derived from human ES cells efficiently engraft in animal models of Parkinson's disease. *Nature* 480(7378):547–551.
15. Giasson BI, Murray IV, Trojanowski JQ, Lee VM (2001) A hydrophobic stretch of 12 amino acid residues in the middle of alpha-synuclein is essential for filament assembly. *J Biol Chem* 276(4):2380–2386.
16. Waxman EA, Mazzulli JR, Giasson BI (2009) Characterization of hydrophobic residue requirements for alpha-synuclein fibrillization. *Biochemistry* 48(40):9427–9436.
17. Cooper AA, et al. (2006) Alpha-synuclein blocks ER-Golgi traffic and Rab1 rescues neuron loss in Parkinson's models. *Science* 313(5785):324–328.
18. Gitler AD, et al. (2008) The Parkinson's disease protein alpha-synuclein disrupts cellular Rab homeostasis. *Proc Natl Acad Sci USA* 105(1):145–150.
19. Credle JJ, et al. (2015) α-Synuclein-mediated inhibition of ATF6 processing into COPII vesicles disrupts UPR signaling in Parkinson's disease. *Neurobiol Dis* 76:112–125.
20. Thayanidhi N, et al. (2010) Alpha-synuclein delays endoplasmic reticulum (ER)-to-Golgi transport in mammalian cells by antagonizing ER/Golgi SNAREs. *Mol Biol Cell* 21(11):1850–1863.
21. Kornfeld S (1986) Trafficking of lysosomal enzymes in normal and disease states. *J Clin Invest* 77(1):1–6.
22. Allan BB, Moyer BD, Balch WE (2000) Rab1 recruitment of p115 into a cis-SNARE complex: programming budding COPII vesicles for fusion. *Science* 289(5478):444–448.
23. Nixon RA, Yang DS, Lee JH (2008) Neurodegenerative lysosomal disorders: A continuum from development to late age. *Autophagy* 4(5):590–599.
24. Shachar T, et al. (2011) Lysosomal storage disorders and Parkinson's disease: Gaucher disease and beyond. *Mov Disord* 26(9):1593–1604.
25. Schöndorf DC, et al. (2014) iPSC-derived neurons from GBA1-associated Parkinson's disease patients show autophagic defects and impaired calcium homeostasis. *Nat Commun* 5:4028.
26. Sardi SP, et al. (2011) CNS expression of glucocerebrosidase corrects alpha-synuclein pathology and memory in a mouse model of Gaucher-related synucleinopathy. *Proc Natl Acad Sci USA* 108(29):12101–12106.
27. Xu YH, et al. (2011) Accumulation and distribution of α-synuclein and ubiquitin in the CNS of Gaucher disease mouse models. *Mol Genet Metab* 102(4):436–447.
28. Cullen V, et al. (2011) Acid β-glucosidase mutants linked to Gaucher disease, Parkinson disease, and Lewy body dementia alter α-synuclein processing. *Ann Neurol* 69(6): 940–953.
29. Sun Y, et al. (2015) Properties of neurons derived from induced pluripotent stem cells of Gaucher disease type 2 patient fibroblasts: potential role in neuropathology. *PLoS One* 10(3):e0118771.
30. Fishbein I, Kuo YM, Giasson BI, Nussbaum RL (2014) Augmentation of phenotype in a transgenic Parkinson mouse heterozygous for a Gaucher mutation. *Brain* 137(Pt 12): 3235–3247.
31. Solano SM, Miller DW, Augood SJ, Young AB, Penney JB, Jr (2000) Expression of alpha-synuclein, parkin, and ubiquitin carboxy-terminal hydrolase L1 mRNA in human brain: Genes associated with familial Parkinson's disease. *Ann Neurol* 47(2):201–210.
32. Miller DW, et al. (2005) Absence of alpha-synuclein mRNA expression in normal and multiple system atrophy oligodendroglia. *J Neural Transm (Vienna)* 112(12):1613–1624.
33. Rocha EM, et al. (2015) Progressive decline of glucocerebrosidase in aging and Parkinson's disease. *Ann Clin Transl Neurol* 2(4):433–438.
34. Chung CY, et al. (2013) Identification and rescue of α-synuclein toxicity in Parkinson patient-derived neurons. *Science* 342(6161):983–987.
35. Cuervo AM, Stefanis L, Fredenburg R, Lansbury PT, Sulzer D (2004) Impaired degradation of mutant alpha-synuclein by chaperone-mediated autophagy. *Science* 305(5688):1292–1295.
36. Martinez-Vicente M, et al. (2008) Dopamine-modified alpha-synuclein blocks chaperone-mediated autophagy. *J Clin Invest* 118(2):777–788.
37. Moyer BD, Allan BB, Balch WE (2001) Rab1 interaction with a GM130 effector complex regulates COPII vesicle cis-Golgi tethering. *Traffic* 2(4):268–276.
38. McGlinchey RP, Lee JC (2015) Cysteine cathepsins are essential in lysosomal degradation of α-synuclein. *Proc Natl Acad Sci USA* 112(30):9322–9327.
39. Webb JL, Ravikumar B, Atkins J, Skepper JN, Rubinsztein DC (2003) Alpha-Synuclein is degraded by both autophagy and the proteasome. *J Biol Chem* 278(27):25009–25013.